

## Ensuring Homology between 2D and 3D Molecular Crystals

Hung Dang,<sup>\*,†</sup> Thierry Maris,<sup>†</sup> Ji-Hyun Yi,<sup>‡</sup> Federico Rosei,<sup>§</sup> Antonio Nanci,<sup>‡</sup> and James D. Wuest<sup>\*,†</sup>

Département de Chimie and Faculté de Médecine Dentaire, Université de Montréal, Montréal, Québec H3C 3J7, and Centre Énergie, Matériaux et Télécommunications, Institut National de la Recherche Scientifique, 1650 Boulevard Lionel-Boulet, Varennes, Québec J3X 1S2, Canada

Received September 18, 2007

Integrated studies using scanning tunneling microscopy and X-ray crystallography have established that 4,5,9,10-tetrahydropyrene-2,7-dicarboxylic acid and pyrene-2,7-dicarboxylic acid crystallize in 2D and 3D with striking homology. Different behavior is shown by related biphenyls that lack the planarizing conformational constraints of the pyrenyl core and the directing effects of intermolecular hydrogen bonding. The results of these studies show that molecules specifically designed to engage in multiple strong directional interadsorbate interactions are promising tools for imposing particular nanopatterns on surfaces and for revealing subtle aspects of crystallization.

### Introduction

One of the greatest current challenges in materials science is learning how the structure and properties of individual molecules are related to those of their aggregates. Mastery of this relationship will allow new molecular materials to be made by design, thereby creating opportunities for breakthroughs in many areas of technology. Unfortunately, full understanding remains elusive, in part because intermolecular interactions are typically weak, complex, and difficult to predict.

A special class of materials with properties more easily foreseen can be built from subunits called tectons,<sup>1</sup> which are molecules that engage in multiple strong directional interactions, such as hydrogen bonds. In favorable cases, the association of tectons induces the assembly of networks in which each molecule is positioned predictably with respect to its neighbors.<sup>2,3</sup> This strategy has become a productive source of molecular crystals with predefined structures and properties, as well as of designed materials with lower degrees of order such as gels, liquid crystals, and even glasses.<sup>4</sup> Here, we show that this strategy can also provide predictably ordered arrays of molecules physisorbed on surfaces at the solid–liquid interface, and we demonstrate that studying two-dimensional (2D) and three-dimensional (3D) crystallization in close tandem is a powerful way to acquire a deeper understanding of molecular self-assembly.

Assembly on surfaces is controlled by interactions within the adsorbed layer and between the adsorbates and the underlying surface. Tectons offer an opportunity to increase the importance of programmed interadsorbate interactions relative to more diffuse adsorbate–surface interactions, making them attractive for creating predictable nanopatterns on surfaces. Earlier studies of ordered adsorption on highly oriented pyrolytic graphite (HOPG) at the solid–liquid interface have included examples of molecules that form hydrogen bonds,<sup>5,6</sup> in most cases, however, the adsorbates also incorporate multiple long alkyl chains,<sup>5</sup> which

have an affinity for HOPG and align preferentially with specific directions on the surface. Reports of the adsorption of hydrogen-bonding molecules without such chains are rare,<sup>6</sup> and the unique advantages of using simple tectons to nanopattern surfaces have not been fully revealed.

### Experimental Section

**2,7-Dibromo-4,5,9,10-tetrahydropyrene.**<sup>7</sup> A solution of 4,5,9,10-tetrahydropyrene (1.0 g, 4.8 mmol)<sup>8a</sup> in chloroform (15 mL) was cooled to 0 °C under Ar for 30 min, and Al powder (spatula tip, ~20–25 mg) was added in one portion. The resulting suspension was stirred for 10 min. Br<sub>2</sub> (1.7 g, 11 mmol) was added to the mixture dropwise, followed by more Al powder (10–15 mg). The orange-brown mixture turned cloudy, a precipitate was formed, and HBr gas was evolved. The mixture was stirred for 2 h at 0 °C under Ar, and then chloroform (50 mL) was added to dissolve the precipitate. The mixture was washed three times with saturated aqueous Na<sub>2</sub>SO<sub>3</sub> to remove excess Br<sub>2</sub>. The organic phase was then washed three times with 1 M aqueous NaOH to remove residual HBr, with deionized water (three times), and then with brine (once). The organic phase was then dried over anhydrous Na<sub>2</sub>SO<sub>4</sub>. The clear colorless solution was filtered, and volatiles were removed by evaporation under reduced pressure to afford 2,7-dibromo-4,5,9,10-tetrahydropyrene, a known compound,<sup>7</sup> as a crystalline beige solid in near-

(5) For recent examples, see: (a) Lena, S.; Brancolini, G.; Gottarelli, G.; Mariani, P.; Masiero, S.; Venturini, A.; Palermo, V.; Pandoli, O.; Pieraccini, S.; Samorì, P.; Spada, G. P. *Chem.—Eur. J.* **2007**, *13*, 3757–3764. (b) Nath, K. G.; Ivasenko, O.; Miwa, J. A.; Dang, H.; Wuest, J. D.; Nanci, A.; Perepichka, D. F.; Rosei, F. *J. Am. Chem. Soc.* **2006**, *128*, 4212–4213. (c) Tao, F.; Bernasek, S. L. *J. Am. Chem. Soc.* **2005**, *127*, 12750–12751. (d) Otsuki, J.; Nagamine, E.; Kondo, T.; Iwasaki, K.; Asakawa, M.; Miyake, K. *J. Am. Chem. Soc.* **2005**, *127*, 10400–10405. (e) De Feyter, S.; Miura, A.; Yao, S.; Chen, Z.; Würthner, F.; Jonkheijm, P.; Schenning, A. P. H. J.; Meijer, E. W.; De Schryver, F. C. *Nano Lett.* **2005**, *5*, 77–81. (f) Wasserfallen, D.; Fischbach, I.; Chebotareva, N.; Kastler, M.; Pisula, W.; Jäckel, F.; Watson, M. D.; Schnell, I.; Rabe, J. P.; Spiess, H. W.; Müllen, K. *Adv. Funct. Mater.* **2005**, *15*, 1585–1594.

(6) (a) Perdígão, L. M. A.; Champness, N. R.; Beton, P. H. *Chem. Commun.* **2006**, 538–540. (b) Kampschulte, L.; Lackinger, M.; Maier, A.-K.; Kishore, R. S. K.; Griessl, S.; Schmittel, M.; Heckl, W. M. *J. Phys. Chem. B* **2006**, *110*, 10829–10836. (c) Lackinger, M.; Griessl, S.; Heckl, W. M.; Hietschold, M.; Flynn, G. W. *Langmuir* **2005**, *21*, 4984–4988. (d) Stepanow, S.; Lin, N.; Vidal, F.; Landa, A.; Ruben, M.; Barth, J. V.; Kern, K. *Nano Lett.* **2005**, *5*, 901–904. (e) Clair, S.; Pons, S.; Seitsonen, A. P.; Brune, H.; Kern, K.; Barth, J. V. *J. Phys. Chem. B* **2004**, *108*, 14585–14590. (f) Lackinger, M.; Griessl, S.; Markert, T.; Jamitzky, F.; Heckl, W. M. *J. Phys. Chem. B* **2004**, *108*, 13652–13655. (g) Lu, J.; Lei, S.-b.; Zeng, Q.-d.; Kang, S.-z.; Wang, C.; Wan, L.-j.; Bai, C.-l. *J. Phys. Chem. B* **2004**, *108*, 5161–5165.

(7) (a) Porwisiak, J.; Dmowski, W. *Synth. Commun.* **1989**, *19*, 3221–3229. (b) Lee, H.; Harvey, R. G. *J. Org. Chem.* **1986**, *51*, 2847–2848.

(8) (a) Connor, D. M.; Allen, S. D.; Collard, D. M.; Liotta, C. L.; Schiraldi, D. A. *J. Org. Chem.* **1999**, *64*, 6888–6890. (b) Rowsell, J. L. C.; Yaghi, O. M. *J. Am. Chem. Soc.* **2006**, *128*, 1304–1315.

\* Authors to whom correspondence may be addressed: james.d.wuest@umontreal.ca; dang@chem.ucla.edu.

<sup>†</sup> Département de Chimie, Université de Montréal.

<sup>‡</sup> Faculté de Médecine Dentaire, Université de Montréal.

<sup>§</sup> Institut National de la Recherche Scientifique.

(1) Simard, M.; Su, D.; Wuest, J. D. *J. Am. Chem. Soc.* **1991**, *113*, 4696–4698.

(2) Wuest, J. D. *Chem. Commun.* **2005**, 5830–5837.

(3) Hosseini, M. W. *Acc. Chem. Res.* **2005**, *38*, 313–323.

(4) For examples, see: (a) Lebel, O.; Maris, T.; Perron, M.-È.; Demers, E.; Wuest, J. D. *J. Am. Chem. Soc.* **2006**, *128*, 10372–10373. (b) Maly, K. E.; Dauphin, C.; Wuest, J. D. *J. Mater. Chem.* **2006**, *16*, 4695–4700.

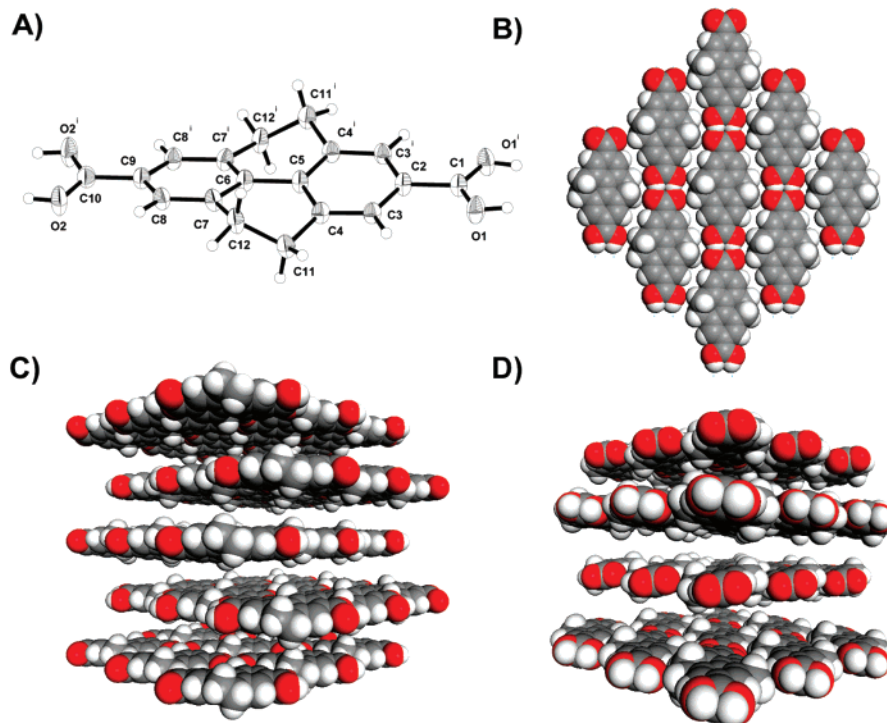


**Figure 1.** (A) Thermal displacement ellipsoid plot of the chiral structure of tecton **1a**, with thermal ellipsoids drawn at the 50% probability level and hydrogen atoms represented by spheres of arbitrary size. The hydrogen atoms of the COOH groups are disordered, with an occupancy of 0.5. (B) Model of the structure viewed along the *c*-axis, revealing a homochiral sheet built from close-packed hydrogen-bonded chains. Atoms of C, H, and O are colored gray, white, and red, respectively. (C) Cross-sectional view perpendicular to the *c*-axis, showing five nonadjacent sheets with the four intervening sheets removed for clarity. (D) View showing that the four intervening sheets are rotated by 90°.

quantitative yield. The product was deemed sufficiently pure for immediate use in the next step:  $^1\text{H NMR}$  (400 MHz,  $\text{CDCl}_3$ )  $\delta$  2.82 (s, 8H, benzylic), 7.21 (s, 4H, aromatic);  $^{13}\text{C NMR}$  (100 MHz,  $\text{CDCl}_3$ )  $\delta$  137.09, 128.90, 128.86, 120.82, 27.82.

**4,5,9,10-Tetrahydropyrene-2,7-dicarboxylic Acid (1a).**<sup>8a</sup> In a flame-dried 100 mL flask, 2,7-dibromo-4,5,9,10-tetrahydropyrene (0.50 g, 1.4 mmol) was dissolved in anhydrous THF (50 mL) under  $\text{N}_2$ , and the solution was kept at  $-78^\circ\text{C}$  for 30 min. Excess *n*-BuLi (7.2 mL, 1.6 M in hexane, 12 mmol) was then added dropwise. During the addition, the initial yellow solution turned darker, and a colorless precipitate was formed. The mixture was stirred at  $-78^\circ\text{C}$  for 30–45 min under  $\text{N}_2$ , and then excess  $\text{CO}_2$  gas (dry ice in a 1 L round-bottom flask) was bubbled into the solution by cannula. The resulting mixture was stirred at  $-78^\circ\text{C}$  and then allowed to warm slowly to room temperature overnight. Deionized water (50 mL) was then added, the mixture was concentrated by partial evaporation under reduced pressure, and the residual aqueous phase was acidified with 1 M aqueous HCl to give a cloudy, pale yellow suspension. The solid was separated by filtration, then washed with water, hexane, ethyl acetate, and ether, and finally dried to afford 4,5,9,10-tetrahydropyrene-2,7-dicarboxylic acid (**1a**); 0.39 g, 1.3 mmol, 93%), a known compound,<sup>8a</sup> as an off-white solid:  $^1\text{H NMR}$  (400 MHz,  $\text{DMSO}-d_6$ )  $\delta$  2.89 (s, 8H, benzylic), 7.72 (s, 4H, aromatic), 12.75 (s, 2H, COOH);  $^{13}\text{C NMR}$  (100 MHz,  $\text{DMSO}-d_6$ )  $\delta$  167.32, 135.99, 133.29, 130.04, 127.15, 27.28.

**Pyrene-2,7-dicarboxylic Acid (2a).**<sup>8</sup> The synthetic procedure for making pyrene-2,7-dicarboxylic acid (**2a**) was analogous to that used to prepare tetrahydropyrene **1a**. To a solution of 2,7-dibromopyrene (0.26 g, 0.72 mmol)<sup>7b</sup> in THF (50 mL) at  $-78^\circ\text{C}$  under  $\text{N}_2$ , excess *n*-BuLi (3.6 mL, 1.6 M in hexane, 5.8 mmol) was added dropwise, followed by  $\text{CO}_2$  gas. This yielded pyrene-2,7-dicarboxylic acid (**2a**); 0.20 g, 0.69 mmol, 96%), a known compound,<sup>8b</sup> as a bright yellow solid:  $^1\text{H NMR}$  (400 MHz,  $\text{DMSO}-d_6$ )  $\delta$  8.39 (s, 4H), 8.91 (s, 4H), 13.38 (s, 2H, COOH).

**Single-Crystal X-ray Diffraction.** Single crystals of tecton **1a** were grown from a saturated solution in DMSO. A light yellow,

football-shaped crystal (0.22 mm  $\times$  0.22 mm  $\times$  0.12 mm) was cooled under a stream of  $\text{N}_2$  gas at 150(2) K, and diffraction data were collected using Cu  $K\alpha$  radiation on a Bruker Microstar diffractometer system. Analysis revealed that the crystal belonged to the tetragonal space group  $P4_32_12$  with  $a = b = 9.7778(2)$  Å,  $c = 14.0111(5)$  Å,  $V = 1339.54(6)$  Å<sup>3</sup>, and  $Z = 2$ . A total of 14136 reflections were collected in the range  $5.52^\circ < 2\theta < 66.74^\circ$ , of which 1196 [ $R_{\text{int}} = 0.080$ ] were independent reflections. The Bruker *SHELXTL* program was used to solve the structure by direct methods (*SHELXS-97*).<sup>9</sup> The structure was refined by a weighted full-matrix least-squares procedure with *SHELXL-97*<sup>9</sup> using  $F_o^2$  data to give final residual factors  $R_1 = 0.0548$  and  $wR_2 = 0.1349$  ( $I > 2\sigma[I]$ ). All non-hydrogen atoms were refined anisotropically, whereas hydrogen atoms were placed in ideal positions and defined as riding atoms. The refined Flack parameter converged to a value of 0.56(2), indicating the presence of a racemic twin.<sup>10</sup> Hydrogen atoms of the COOH groups were statistically disordered over the two oxygen atoms with occupancy factors of 0.5.

Crystals of 4,5,9,10-tetrahydropyrene were grown by slow evaporation of a saturated solution in ether. Large, colorless, flat prisms were obtained (0.60 mm  $\times$  0.35 mm  $\times$  0.18 mm), and X-ray analysis was performed at 296(2) K. The crystals were determined to belong to the orthorhombic space group  $P2_12_12_1$  with  $a = 8.0049(4)$  Å,  $b = 8.5815(4)$  Å,  $c = 32.3805(16)$  Å,  $V = 2224.35(19)$  Å<sup>3</sup>, and  $Z = 8$ . A total of 12852 reflections were collected in the range  $2.73^\circ < 2\theta < 73.11^\circ$ , of which 4384 [ $R_{\text{int}} = 0.046$ ] were independent reflections. All stages of weighted full-matrix least-squares refinement were performed using  $F_o^2$  data, which converged to give  $R_1 = 0.0418$  and  $wR_2 = 0.0906$  ( $I > 2\sigma[I]$ ).

Additional X-ray crystallographic data for compound **1a** and 4,5,9,10-tetrahydropyrene, including ORTEP drawings, tables of

(9) Sheldrick, G. M. *SHELXS-97, Program for the Solution of Crystal Structures and SHELXL-97, Program for the Refinement of Crystal Structures*; Universität Göttingen: Germany, 1997.

(10) Flack, H. D.; Schwarzenbach, D. *Acta Crystallogr.* **1988**, *A44*, 499–506. Flack, H. D. *Acta Crystallogr.* **1983**, *A39*, 876–881.

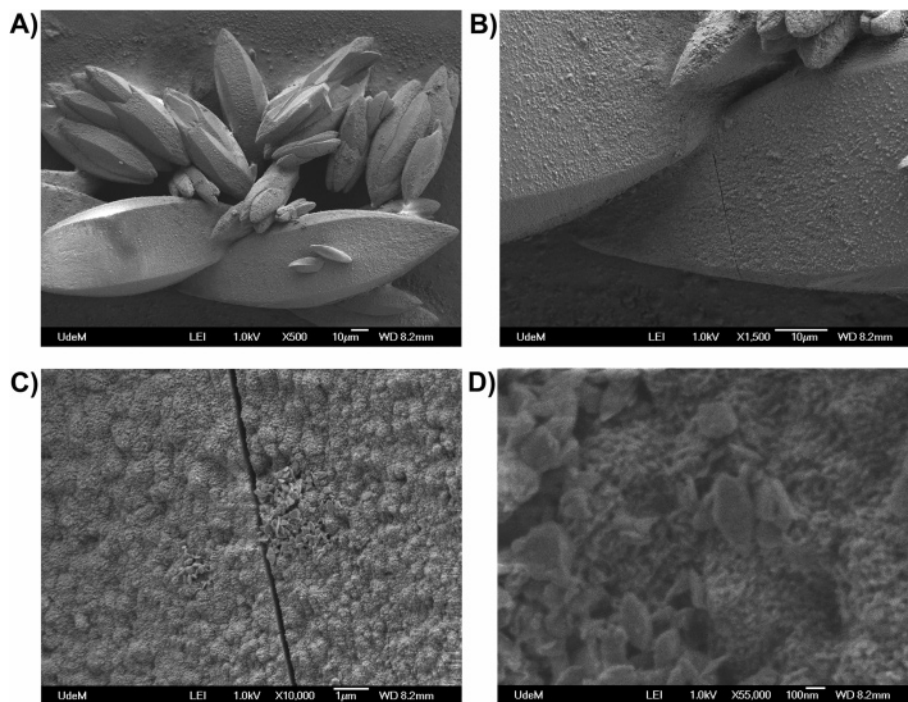


**Figure 2.** High-resolution scanning electron micrographs showing crystals of tecton **1a** grown from DMSO. (A) Clusters of football-shaped single crystals were observed with the long axis corresponding to the *c*-axis of the crystallographic unit cell. Zoomed-in images (B,C) reveal a clean fracture line perpendicular to the *c*-axis, between the 2D sheets formed by tecton **1a**. (D) Microcrystals can be seen to aggregate on the major face of the mature crystal.

structural data, and CIF files, are provided as Supporting Information.

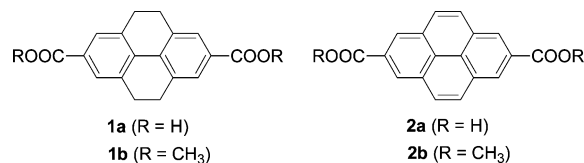
**Scanning Electron Microscopy (SEM).** Single crystals of tecton **1a** were removed from the mother liquors and placed on a graphite disk. Adhering solvent was removed by evaporation under reduced pressure. The mounted sample was observed at 25 °C using a high-resolution JEOL JSM-7400F field-emission scanning electron microscope operated at 1 kV. The SEM images shown in Figure 2 are presented without further processing.

**Scanning Tunneling Microscopy (STM).** All STM experiments were performed at room temperature (20–25 °C). All solvents used for STM studies (heptanoic acid, 1,2,4-trichlorobenzene, 1-undecanol, 1-phenyloctane, 1-octanol) were purchased from Aldrich and used as received. STM experiments for tectons **1a** and **2a** were performed using a JEOL JSPM-5200 instrument equipped with a narrow scanner. Platinum/iridium STM tips (Pt/Ir, 80%/20%, diameter = 0.2 mm) were cut mechanically with a wire cutter. Prior to imaging, tecton **1a** was suspended in heptanoic acid. Tecton **2a** was suspended in a mixture of heptanoic acid, 1,2,4-trichlorobenzene, and 1-undecanol in amounts equivalent to concentrations of approximately  $10^{-4}$  M. For a typical experiment, the freshly cleaved surface of HOPG (Structure Probe, Inc., SPI-1 grade) was first imaged to determine the quality of the Pt/Ir tip and the smoothness of the graphite surface. Once this was determined, a drop of the solution containing tecton **1a** and/or **2a** was applied. The STM investigations were then carried out at the liquid–solid interface in the constant-height mode. STM imaging was performed by changing the tunneling parameters (voltage applied to the tip and the average tunneling current). Raw STM images were processed using a JEOL software package (*WinSPM DPS* software version 2.01, R. B. Leane, JEOL Ltd.) and a freeware (*WSxM 4.0 Develop 8.21*, Nanotec Electronica S. L., August 2005).

## Results and Discussion

To evaluate the special potential of tectons as agents for nanopatterning surfaces in predictable ways, we used X-ray crystallography and scanning tunneling microscopy (STM) at the liquid/HOPG interface to study the 3D and 2D crystallization

of 4,5,9,10-tetrahydropyrene-2,7-dicarboxylic acid (**1a**),<sup>8a</sup> pyrene-2,7-dicarboxylic acid (**2a**),<sup>8b</sup> and related compounds.



Crystals of tetrahydropyrene **1a** were grown by slow evaporation of a solution in DMSO, and their structure was determined by X-ray diffraction. The crystals proved to exist as racemic twins belonging to the chiral tetragonal space group  $P4_32_12$ . In the structure, individual molecules adopt the chiral conformation shown in Figure 1A (and its enantiomer), in which the torsional angle C4–C5–C6–C7 is 15.8(3)°. The intramolecular C1–C10 distance between carbonyl groups is 1.00(1) nm. As expected, normal intermolecular hydrogen bonding of the COOH groups directs the formation of chains, which then pack closely to form sheets perpendicular to the *c*-axis (Figure 1B–D). Each sheet is composed of a single enantiomer of tecton **1a**, but the crystals consist of equal numbers of homochiral sheets of opposite configuration. Crystals of tecton **1a** can be cleaved selectively perpendicular to the *c*-axis (Figure 2). This confirms that molecular adhesion within the sheets, which is maintained in part by hydrogen bonding, is stronger than intersheet adhesion, which involves diffuse interactions. Together, these observations suggest that the distinctive sheets in 3D crystals of tetrahydropyrene **1a** express a strong underlying predisposition to form a homologous 2D pattern on surfaces.

Both the nearly planar tetrahydropyrenyl core and the self-associating COOH groups appear to be prerequisites for the formation of sheets. In derivatives of biphenyl that lack the same planarizing conformational constraints, the angle between the aryl rings is normally close to 40°, and packing obeys a

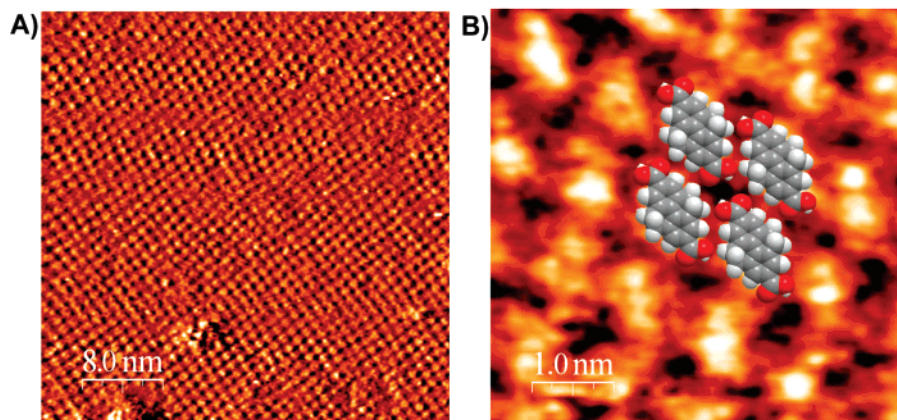


**Figure 3.** (A) STM image of the 2D crystallization of tecton **1a** on HOPG (deposition from heptanoic acid, with  $I_{\text{set}} = 0.055$  nA,  $V_{\text{bias}} = -1.394$  V). (B) High-resolution STM image with a model of the packing superimposed ( $I_{\text{set}} = 0.045$  nA,  $V_{\text{bias}} = -1.513$  V).

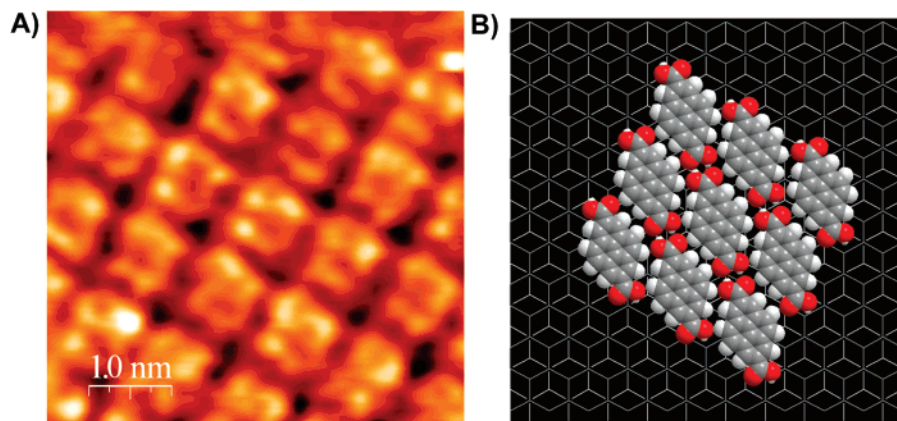


**Figure 4.** (A) STM image of the 2D crystallization of tecton **2a** on HOPG (deposition from a mixture of heptanoic acid, 1-undecanol, and 1,2,4-trichlorobenzene, with  $I_{\text{set}} = 0.065$  nA,  $V_{\text{bias}} = -1.814$  V, image size =  $5.0 \times 5.0$  nm<sup>2</sup>). (B) Model of the packing superimposed on graphite in an arbitrary orientation.

herringbone motif. In particular, 4,4'-biphenyldicarboxylic acid and its diesters crystallize with torsional angles exceeding  $35^\circ$ .<sup>11</sup> Moreover, we have found that 4,5,9,10-tetrahydropyrene itself crystallizes in a herringbone motif, and sheets like those of diacid **1a** are absent. Despite extensive effort, we have not been able to grow crystals of pyrenedicarboxylic acid **2a** suitable for X-ray diffraction; however, its enforced planarity should strongly favor the formation of hydrogen-bonded sheets analogous to those generated by tetrahydropyrene **1a**.

In a typical 2D crystallization, a droplet of a saturated solution of tetrahydropyrene **1a** in heptanoic acid was placed on freshly cleaved HOPG at  $25^\circ\text{C}$ , and the resulting physisorbed assembly was imaged by STM in the constant-height mode (Figure 3). Figure 3A reveals uniformly close-packed domains of large dimensions ( $40 \times 40$  nm<sup>2</sup>). From line-profile analyses, the longer molecular axis is  $\sim 1.0$  nm, which matches the measured intramolecular separation of the carbonyl groups in 3D crystals of compound **1a**. Comparison of Figures 1B and 3B establishes that tecton **1a** crystallizes in 2D and 3D with impressive homology. Our STM images provided no evidence of separate homochiral domains, so physisorption may induce tetrahydropyrene **1a** to adopt a planar achiral conformation, or the rate of interconversion of adsorbed enantiomers ( $E_a = \sim 4\text{--}5$  kcal/mol)<sup>12</sup> may be fast under the experimental conditions.

It is noteworthy that deposition from dilute solutions in heptanoic acid, a solvent able to engage in hydrogen bonding, does not prevent dicarboxylic acid **1a** from self-associating to form the expected sheets on HOPG. Moreover, STM images provided no evidence that heptanoic acid and tecton **1a** coadsorb, even at the periphery of domains. We conclude that the inherent affinity of HOPG for heptanoic acid is substantially lower than for compound **1a**. Furthermore, we note that association of a monocarboxylic acid such as heptanoic acid, according to the cyclic doubly hydrogen-bonded motif characteristic of the COOH group, cannot yield nanopatterns maintained by extended networks of hydrogen bonds, as is possible when the adsorbate incorporates multiple COOH groups. This underscores the profound difference in behavior between tectons and normal molecules unable to engage in multiple strong directional interactions.

As anticipated, analogous pyrenedicarboxylic acid **2a** produced a closely similar nanopattern on HOPG (Figure 4). Unlike domains characteristic of highly alkylated compounds,<sup>5</sup> those formed by tectons **1a** and **2a** showed no preferred orientation on the underlying HOPG. Exposure of HOPG to closely related models, including 4,5,9,10-tetrahydropyrene and dimethyl esters **1b**<sup>8a</sup> and **2b**,<sup>8b</sup> did not yield ordered structures that could be imaged by STM under similar conditions. Together, these observations support three key hypotheses: (1) Tectons **1a** and **2a** are strongly disposed by design to favor the assembly of similar sheets in 2D and 3D; (2) the defining characteristic that distinguishes tectons **1a** and **2a** from model compounds such as 4,5,9,10-tetrahydro-

(11) (a) Kamitori, S.; Muraoka, S.; Kondo, S.; Okuyama, K. *Carbohydr. Res.* **1998**, *312*, 177–181. (b) Li, X.; Brisse, F. *Macromolecules* **1994**, *27*, 7718–7724.

(12) Iwaizumi, M.; Isobe, T. *Bull. Chem. Soc. Jpn.* **1965**, *38*, 1547–1552.

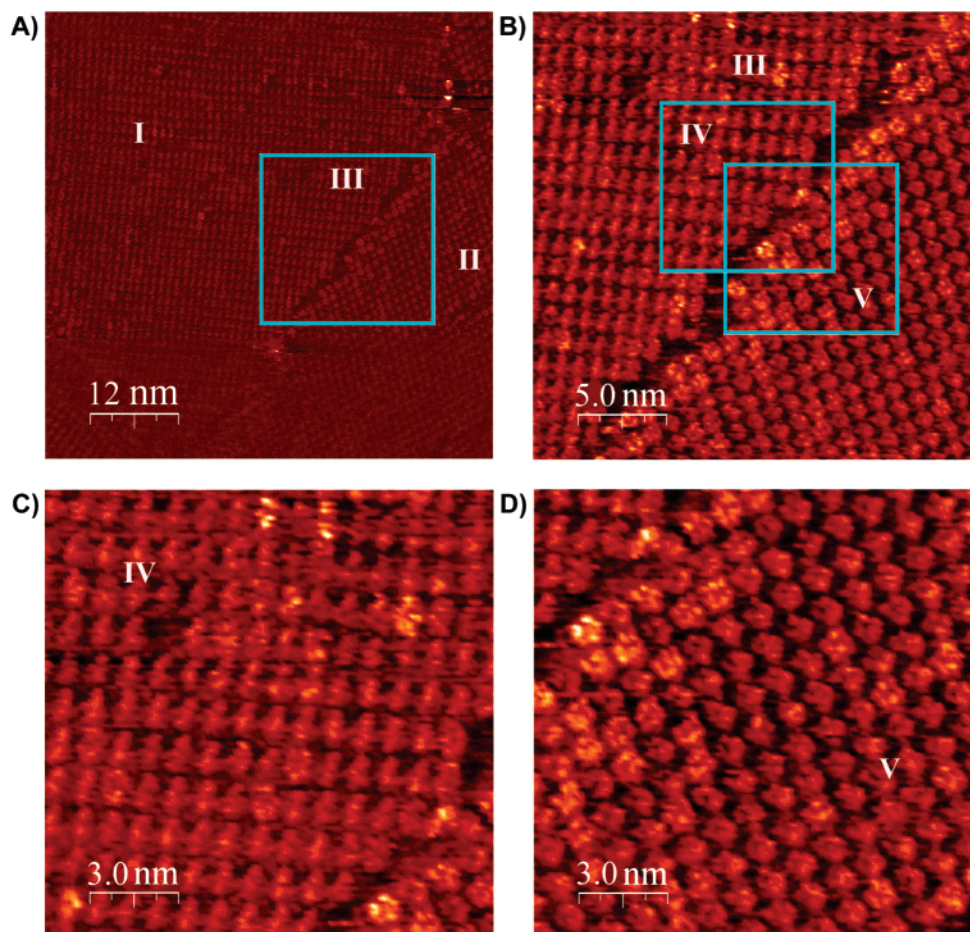


**Figure 5.** STM images of the codeposition of tectons **1a** and **2a** (1:1 mixture in heptanoic acid) on freshly cleaved surfaces of HOPG, using typical bias voltages and tunneling currents of  $I_{\text{set}} = 100$  to  $55$  pA and  $V_{\text{bias}} = -1.5$  to  $-2.0$  V. (A) Tectons **1a** and **2a** self-associate to form segregated domains with large dimensions ( $60 \times 60$  nm<sup>2</sup>). Separate domains formed by tecton **1a** (region I) and tecton **2a** (region II) were observed to coexist in the same image. Region I consists of hydrogen-bonded linear chains of tecton **1a** related to those normally observed when the pure compound is adsorbed (Figure 3).<sup>13</sup> Region II is formed by the analogous self-association of tecton **2a**. (B) A higher-resolution image showing the interfacial zone (region III in Figure 5A) between separate domains formed by tectons **1a** and **2a**. (C,D) Detailed views of regions IV and V clearly illustrate the predisposition of the two tectons to self-associate and to form essentially pure phases.

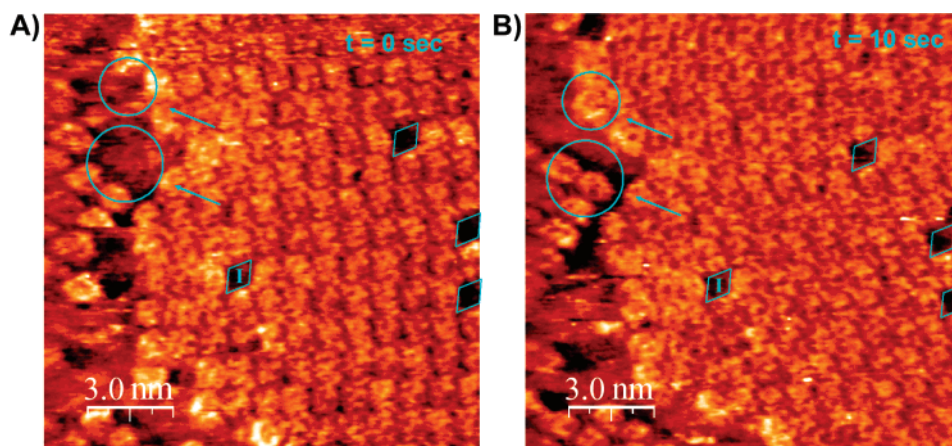


**Figure 6.** (A) Initial STM image of the 2D crystallization of tecton **2a** on HOPG (deposition from a mixture of heptanoic acid, 1-undecanol, and 1,2,4-trichlorobenzene, with  $I_{\text{set}} = 0.055$  nA,  $V_{\text{bias}} = -1.713$  V). (B) STM image after 10 s. In both images, point defects created by missing molecules are marked by diamonds to serve as reference points. Assembly at the interface of the domains is highlighted by circles and arrows.

pyrene and dimethyl esters **1b–2b** is the presence of multiple sites of hydrogen bonding, which help stabilize the 2D crystals and thereby facilitate their imaging; and (3) self-association of tectons **1a** and **2a** is more important in determining the structure of the 2D crystals than is their precise mode of interaction with the surface.

As a result, tectons promise to be uniquely effective tools for imposing particular nanopatterns on atomically flat surfaces with various underlying structures. Moreover, tectons are ideally suited for probing subtle aspects of crystallization. In particular, we have noted that 3D crystallization discriminates tectons **1a** and **2a** with high fidelity, despite their closely similar molecular

structures, and we have failed to obtain cocrystals or alloys. Analogously, 2D crystallization of 1:1 mixtures on HOPG leads to separate domains of the two components in essentially pure form (Figure 5). By demonstrating that extensive lattice substitution is difficult in both 2D and 3D, even using molecules with very similar structures, these experiments provide further evidence of homology in 2D and 3D crystallization.

Detailed examination of STM images of coadsorption revealed that individual domains can nevertheless accommodate occasional substitutional defects, particularly near boundaries, in which the incorrect tecton is oriented in a way that maintains proper hydrogen bonding.<sup>13</sup> In addition, time-lapse images of the boundaries of pure 2D crystals (Figure 6) revealed that new molecules add to specific edge sites at rates much faster than internal defects are repaired. In addition, the images suggest that such additions occur preferentially by forming new hydrogen bonds, rather than merely van der Waals contacts.

### Conclusions

Tectons have already proven to be a prolific source of 3D crystals with predictable structural features and novel properties. The present results underscore their special potential for creating predetermined 2D assemblies on surfaces. In addition, the work

illustrates the special value of tightly integrated studies in which 2D and 3D crystallization are examined simultaneously and in which structural hypotheses are reinforced by the synthesis and analysis of appropriate models. Together, our results suggest that tectons will be indispensable tools in surface science, because they can maximize directional interadsorbate adhesion relative to diffuse interactions with surfaces and neighboring adsorbates. As we have begun to demonstrate, these properties can be exploited to clarify puzzling aspects of crystallization in molecular detail, including the formation of cocrystals and molecular alloys, the nature of defects, and the growth and repair of crystals in both 2D and 3D.

**Acknowledgment.** We are grateful to the Natural Sciences and Engineering Research Council of Canada, the Canadian Institutes of Health Research, the Ministère de l'Éducation du Québec, the Canada Foundation for Innovation, and the Canada Research Chairs Program for financial support. We thank Sylvia F. Zalzal for helping us acquire SEM images.

**Supporting Information Available:** Additional X-ray crystallographic data for compound **1a** and 4,5,9,10-tetrahydropyrene, including ORTEP drawings, tables of structural data, and CIF files; additional STM images of compounds **1a** and **2a**. This material is available free of charge via the Internet at <http://pubs.acs.org>.

LA702885Y

---

(13) See the Supporting Information for details.